

Recombinant Lhca2 and Lhca3 Subunits of the Photosystem I Antenna System

Simona Castelletti,^{‡,§,||} Tomas Morosinotto,^{‡,||} Bruno Robert,[§] Stefano Caffarri,^{‡,⊥} Roberto Bassi,^{‡,⊥} and Roberta Croce^{*,#}

Dipartimento Scientifico e Tecnologico, Università di Verona, Strada Le Grazie, 15- 37234 Verona, Italy, Service de Bioénergétique, Bât. 532 CEA-Saclay, 91191 Gif-sur-Yvette, France, Université Aix-Marseille II, LGBP (Laboratoire de Genetique et Biophysique des Plantes) Faculté des Sciences de Luminy, Département de Biologie, Case 901-163, Avenue de Luminy-13288 Marseille, France, and Istituto di Biofisica, CNR sezione di Milano, c/o Dipartimento di Biologia, Via Celoria 26, 20133 Milano, Italy

Received December 20, 2002; Revised Manuscript Received February 14, 2003

ABSTRACT: In this study, two gene products (Lhca2 and Lhca3), encoding higher plants (*Arabidopsis thaliana*) Photosystem I antenna complexes, were overexpressed in bacteria and reconstituted in vitro with purified chloroplast pigments. The chlorophyll-xanthophyll proteins thus obtained were characterized by biochemical and spectroscopic methods. Both complexes were shown to bind 10 chlorophyll (*a* and *b*) molecules per polypeptide, Lhca2 having higher chlorophyll *b* content as compared to Lhca3. The two proteins differed for the number of carotenoid binding sites: two and three for Lhca2 and Lhca3, respectively. β -carotene was specifically bound to Lhca3 in addition to the xanthophylls violaxanthin and lutein, indicating a peculiar structure of carotenoid binding sites in this protein since it is the only one so far identified with the ability of binding β -carotene. Analysis of the spectroscopic properties of the two pigment proteins showed the presence of low energy absorption forms (red forms) in both complexes, albeit with different energies and amplitudes. The fluorescence emission maximum at 77 K of Lhca2 was found at 701 nm, while in Lhca3 the major emission was at 725 nm. Reconstitution of Lhca3 without Chl *b* reveals that Chl *b* is not involved in originating the low energy absorption forms of this complex. The present data are discussed in comparison to the properties of the recombinant Lhca1 and Lhca4 complexes and of the native LHCI preparation, previously analyzed, thus showing a comprehensive description of the gene products composing the Photosystem I light harvesting system of *A. thaliana*.

The outer antenna system of higher plant Photosystem I, LHCI,¹ is composed of four proteins (1–3), the products of the genes Lhca1–4 (4), which coordinate Chl *a*, Chl *b*, lutein, violaxanthin, and β -carotene (5, 6). These complexes are present in dimeric form in vivo (7), and they are located on one side of the PSI core complex (8), in connection with PsaF, PsaG, and PsaK subunits (9, 10). The sequence homology with Lhcb proteins suggests that they share structure similarity with LHCII complex (11, 12). Thus, their structure is proposed to include three membrane spanning helices and one amphipathic helix on the luminal side of the membrane.

The purification of each Lhca gene product to homogeneity has proven problematic because of strong interactions between subunits in the heterodimers, which require harsh detergent treatments to be broken, yielding into denaturation.

Most of the studies on the complexes purified from thylakoids membrane have therefore been achieved on heterogeneous preparations containing several polypeptides (3, 7, 13–16) leading to determination of the average properties of the complexes. A possible solution to this problem has been offered by overexpression of the genes in bacterial systems and reconstitution in vitro of the apoproteins with pigments (17). Biochemical and spectroscopic data are now available for Lhca1 and Lhca4 subunits (7, 18–22).

The major characteristic of LHCI is the presence of significant absorption in the low energy side of the spectrum because of Chl spectral forms red-shifted at energies lower than the Photosystem I primary donor, P700. These forms were found to be associated to a LHCI subfraction named LHCI-730, which contains Lhca1 and Lhca4 (3, 13, 14, 23). In vivo and in vitro analyses have demonstrated that the red absorption originates mainly from Chls associated to the Lhca4 subunit (18, 24). The presence of low energy forms in Lhca2 and Lhca3 complexes is more controversial. In the early purifications of LHCI antenna, these two complexes were found in a fraction showing a low-temperature emission peak at 680–690 nm (named LHCI-680) (3, 13, 14, 23). It was argued that no red-shifted Chl forms were associated to these two subunits. More recently, analysis of a LHCI preparation containing all four Lhca proteins revealed the presence of a 702 nm fluorescence emission component that was attributed to Lhca2 and/or Lhca3 dimers (15, 16).

* Author to whom correspondence should be addressed. E-mail: roberta.croce@unimi.it. Tel +39 0250314856. Fax +39 0250314815.

[‡] Università di Verona.

[§] Service de Bioénergétique.

^{||} These authors contributed equally to this work.

[⊥] Université Aix-Marseille II.

[#] Istituto di Biofisica.

¹ Abbreviations: AA, amino acid; b-car, β -carotene; CD, circular dichroism; Car, carotenoid; Chl, chlorophyll; HPLC, high-performance liquid chromatography; Lhc, light harvesting complex; LHCI and LHCII, light harvesting complex of Photosystem I and II; LT, low temperature (77 K); lute, lutein; neo, neoxanthin; PSI, Photosystem I; RT, room temperature; viola, violaxanthin.

Purification of a dimeric fraction enriched in Lhca2 and Lhca3 also suggested that red forms could be associated to these complexes (6, 7). A similar proposal came from the analysis of antisense plants depleted in Lhca2 and Lhca3 subunits (25). In fact, these plants showed a blue-shifted 77 K fluorescence emission spectrum as compared to WT plants and decreased absorption at 695 and 715 nm. The *in vitro* reconstitution of monomeric Lhca2 and Lhca3 appears to confirm the presence of low energy forms in these two subunits (22).

The aim of this work is to provide information on Lhca2 and Lhca3 complexes, which are at present the lesser known antenna proteins of higher plants. In this study, Lhca2 and Lhca3 apoproteins of *Arabidopsis thaliana* overexpressed in *Escherichia coli* were reconstituted *in vitro* with pigments, and the refolded complexes were characterized by biochemical and spectroscopic methods to give a complete picture of their properties. The results are discussed in comparison with the data previously obtained for Lhca1 and Lhca4 and for the native LHCI dimeric preparation (7) with major emphasis on the low energy spectral forms.

MATERIALS AND METHODS

DNA Constructions. Plasmids were constructed using standard molecular cloning procedures (26). cDNA of Lhca2 and Lhca3 from *A. thaliana* were supplied by Arabidopsis Biological Resource Center (ABRC) at the Ohio State University. The coding regions for the putative mature polypeptides were amplified by PCR (Lhca2: forward primer, GGGGTGACAGTCGACAGCTGATCCAG, reverse primer, GGGAAGCTTCTTGGGTGTGAAAGC; Lhca3: forward primer, CGAGGATCCGCTGCAGCTCACCTGTC, reverse primer, CGGAAGCTTGTGGAACCTGAGGCTGGTC). The amplified regions were cloned in the pQE-50 (Qiagen) expression vector.

Isolation of Overexpressed Lhca Apoproteins from Bacteria. Lhca apoproteins were expressed and purified from *E. coli*, using BL21 and SG13009 strains respectively for Lhca2 and Lhca3 constructs, following a protocol previously described (27, 28).

Reconstitution and Purification of Lhca–Pigment Complexes. These procedures were performed as described in (29) with the following modifications: 420 μ g of apoprotein, 240 μ g of chlorophylls, and 35 μ g of carotenoids were used in the reconstitution. The Chl *a/b* ratio in the pigment mixture used for the reconstitution of the control samples was 4. To obtain complexes enriched in Chl *b*, a Chl *a/b* ratio of 0.2 was used. The reconstitution in the absence of Chl *b* was performed with purified Chl *a* from Sigma. All reconstitutions were performed in the presence of all carotenoids of the thylakoid membrane. The pigments used were purified from spinach.

Pigment Analysis. The pigment complement of the holoprotein was analyzed by HPLC (30) and fitting of the absorption spectra of the acetone extracts with the spectra of the individual pigments (31).

Spectroscopy. The absorption spectra at RT were recorded by SLM-Aminco DK2000 spectrophotometer, in 10 mM HEPES pH 7.5, 20% (v/v) glycerol (70% for LT), and 0.06% β -DM, using a step of 0.45 nm. The fluorescence emission spectra were measured on a Jasco FP-777 fluorimeter and

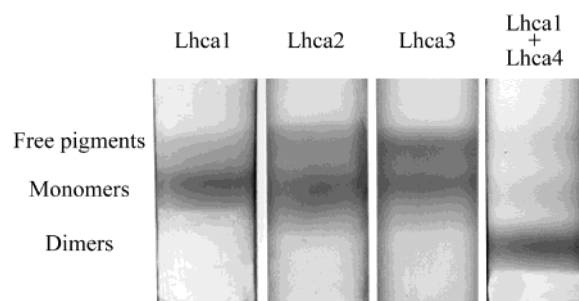


FIGURE 1: Aggregation state of Lhca2 and Lhca3. The mobility of the two complexes upon ultracentrifugation in glycerol density gradient is compared to the mobility of Lhca1 monomer and Lhca1-4 dimer.

corrected for the instrumental response. The samples were excited at 440, 475, and 500 nm. The bandwidths were 5 nm in excitation and 3 nm in emission. For the excitation spectra, the emission was at 700 nm. All fluorescence spectra were measured at 0.02 OD at the maximum of Q_y transition. For the low-temperature measurements, the samples were in 70% glycerol, 10 mM HEPES pH 7.5, 0.03% β -DM.

The CD spectra were measured at 10 °C on a Jasco 600 spectropolarimeter. The samples were in the same solution described for the absorption. All the spectra presented were normalized to the same polypeptide concentration, based on the Chl binding stoichiometry (32).

Denaturation temperature measurements were performed by following the decay of the CD signal at 470 nm when increasing the temperature from 20 to 75 °C with a time slope of 1 °C/min and resolution of 0.2 °C. The thermal stability of the protein was determined by finding the $T_{1/2}$ of the signal decay.

RESULTS

Lhca2 and Lhca3 apoproteins were overexpressed in *E. coli*, and the complexes were reconstituted *in vitro* by refolding in the presence of the full pigment complement extracted from chloroplasts. Both proteins yielded a green band upon sucrose gradient ultracentrifugation. The reconstituted products were then purified from unfolded polypeptides and unspecifically bound pigments by anionic exchange chromatography. The aggregation state of the complexes was investigated by glycerol density gradient ultracentrifugation, a method previously shown to be effective in separating monomers from dimers and free pigments (21). As compared with Lhca1 monomer and Lhca1-4 dimer, Lhca2 and Lhca3 were shown to be obtained in monomeric state (Figure 1).

Pigment Composition. The pigment composition of Lhca2 and Lhca3 was determined by HPLC analysis and fitting of the absorption spectrum of the acetone extracts with the spectra of individual pigments in the same solvent. The results are presented in Table 1. Although the reconstitution of both proteins was performed with the same pigment mixture, the Chl *a/b* ratio was lower in Lhca2 with respect to Lhca3 (1.84 vs 6.0), indicating higher affinity for Chl *b* of the former complex. The Chl/car ratio was also different in the complexes, being 5.0 for Lhca2 and 3.4 for Lhca3. Lutein and violaxanthin were found associated to both proteins, while β -carotene was specifically bound to Lhca3. The neoxanthin, although present in the recon-

Table 1: Pigment Composition of Reconstituted Complexes^a

sample	Chl <i>a/b</i> ratio	Chl/car	Chl <i>b</i>	viola	lute	b-car	Den T (°C)
Lhca2	1.85 ± 0.15	5.0 ± 0.2	54.3 ± 2.9	7.2 ± 1.4	23.5 ± 1.6		53.3 ± 1.9
Lhca3	6.0 ± 0.8	3.5 ± 0.2	16.8 ± 2.0	7.8 ± 0.6	18.9 ± 0.5	6.7 ± 2.3	45.6 ± 1.4

^a The data are the average of four reconstitutions. The values are considered for 100 molecules of Chl *a*.

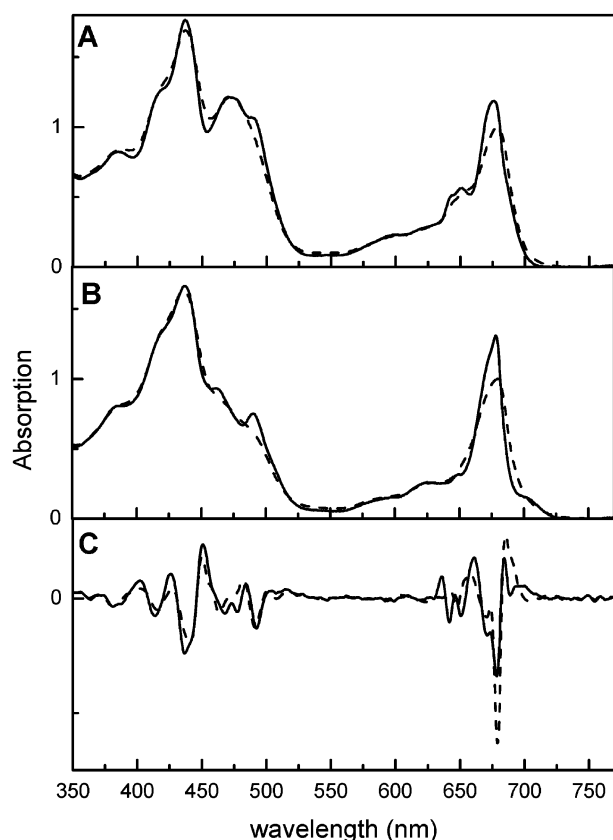


FIGURE 2: Absorption spectra at RT (dashed) and LT (solid) of reconstituted Lhca2 (A) and Lhca3 (B). The spectra are normalized to the total area. In panel C, the second derivative of the spectra at LT is presented: Lhca2 (solid) and Lhca3 (dashed).

stitution mixture, was absent from both complexes in agreement with the composition of native LHCI preparation (7) thus confirming the specificity of the *in vitro* refolding procedure.

Absorption Spectra. The absorption spectra at room temperature (RT) and at 77 K (LT) of the complexes are reported in Figure 2 along with the second derivatives of the LT spectra. The absorption maximum of Lhca2 in the Q_y region was at 676.5 nm (679.0 nm at RT). The second derivative analysis of Lhca2 showed minima at 678.5 nm (682.1 nm at RT), 671 nm (673 nm) in the Q_y region of Chl *a*, and at 651 nm (652.4 nm) and 642 nm (643 nm) in the Chl *b* region. In the blue region of the spectrum, the minimum at 495 nm (492 nm) is related to the carotenoids red most transition and the two minima at 477 and 468 nm to the S_0-S_3 transitions of Chls *b*. In the case of Lhca3, the absorption maximum was at 678.5 nm (679.4 nm at RT), and in the second derivative the values found for the components in Q_y range were of 679 nm (682.1 nm at RT) and 672 nm (671 nm) for Chl *a*, while in the Chl *b* absorption range a small signal was observed at 648 nm (651 nm). In the blue range, Lhca3 showed two signals, at 507 and 491 nm, which can be attributed to carotenoid transitions, while

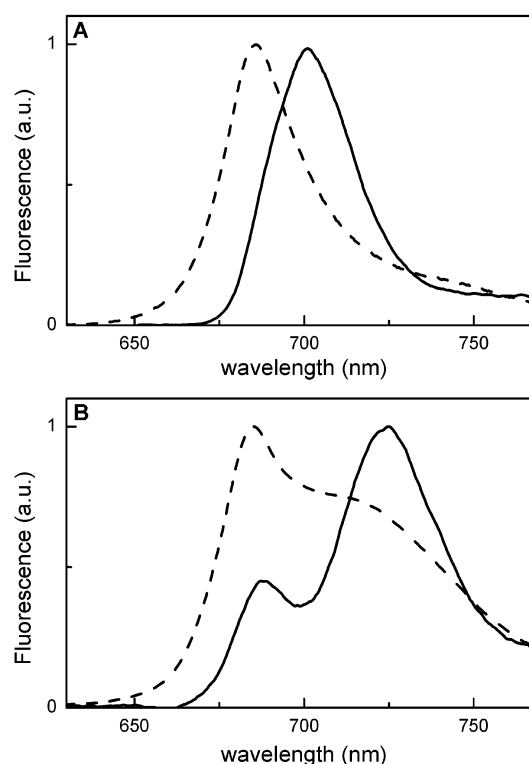


FIGURE 3: Fluorescence emission spectra at RT (dashed) and 77 K (solid) of Lhca2 (A) and Lhca3 (B). The spectra are normalized to the maximum.

components at 475 and 465 nm could be tentatively attributed to different forms of Chl *b* S_0-S_3 transitions. Besides that, the second derivative analysis of the Lhca3 spectrum also showed a 704.6 nm signal, which could not be resolved in the case of Lhca2.

The most interesting feature is the presence of absorption at wavelengths longer than 700 nm, clear indication for red forms in both complexes, albeit with different intensities: the absorption above 700 nm represents at RT the 2.7% (1.1% at LT) of the Q_y absorption in Lhca2 and 5% (5.4% at LT) in Lhca3.

Fluorescence Spectra. The fluorescence emission spectra of the two samples, recorded at RT and 77 K, are shown in Figure 3. At room temperature, Lhca2 fluoresced with a single peak at 688 nm, and the band was asymmetrically broadened, showing contributions at lower energy (Figure 3A). At 77 K, the peak shifted to 701 nm, but a contribution at 688 nm was still present in the high-energy side of this band (Figure 3A). Lhca3 at RT exhibited the emission maximum at 685 nm and strong red emission at wavelengths longer than 705 nm. At low temperature, the spectrum was dominated by a broad signal at 725 nm, while a 688 nm peak was still detectable (Figure 3B). These data are in perfect agreement with the absorption spectra and confirm that both complexes have Chl forms absorbing at low energy.

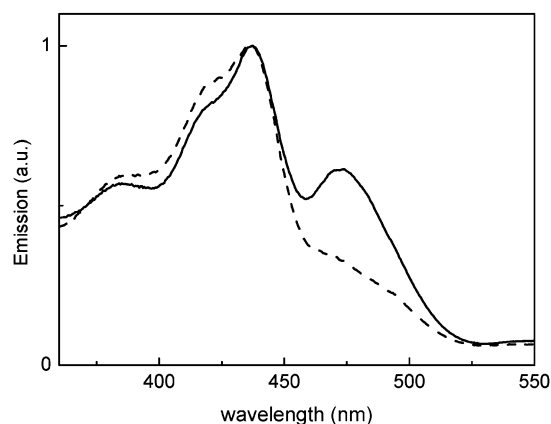


FIGURE 4: Fluorescence excitation spectra of Lhca2 (solid) and Lhca3 (dashed). The spectra are normalized to the maximum.

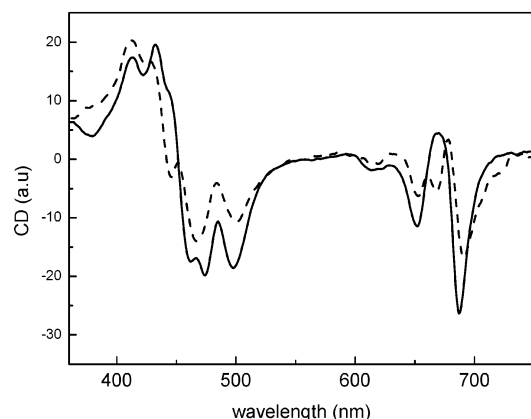


FIGURE 5: CD spectra at RT of Lhca2 (solid) and Lhca3 (dashed). The spectra are normalized to the Chl concentration.

The excitation spectra of the complexes at RT are shown in Figure 4. Comparison between the Soret region of the absorption and the excitation spectrum allowed calculating the carotenoid to chlorophyll energy transfer efficiency in the complexes (31). To this end, the absorption spectra of Lhca2 and Lhca3 were described in terms of sum of absorptions of individual pigments, using the spectra of pigments in protein environment (33). The same description was applied to the excitation spectra: the position of the maxima of the pigments obtained by the analysis of the absorption spectrum was fixed, and only the amplitudes were used as free parameters. The comparison of the areas of the individual pigments in the absorption and excitation spectra yielded the transfer efficiency for each species. The results for Lhca2 indicated an overall carotenoid to Chl energy transfer yield of 75%, a value similar to other Lhc proteins. The error is around 5% assuming for Chl *a* 100% transfer efficiency.

Surprisingly, in Lhca3 the transfer efficiency from carotenoid to Chl was as low as 55%. From the comparison of the absorption and excitation spectra it was observed that a carotenoid absorbing at higher energy (red most peak at 485–489 nm) does not transfer energy to Chl *a*.

CD Spectra. The CD spectra of the two complexes are reported in Figure 5. Lhca2 showed negative components in the Q_y region at 687 and 652 nm and a positive one at 669–670 nm. In the spectrum of Lhca3 complex, three negative signals were present in this range at 691, 668, and 653 nm and a positive one at 678 nm. In this case, a negative

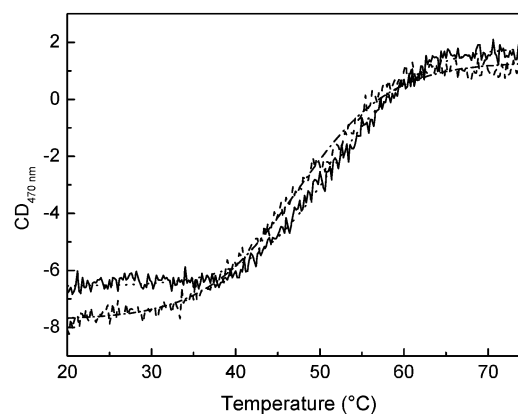


FIGURE 6: CD signal at 470 nm of Lhca2 (solid) and Lhca3 (dotted) vs temperature. The experimental data were fitted with a sigmoidal curve, and the denaturation temperature determinate as $T_{1/2}$.

component at wavelengths longer than 700 nm was also observed, reflecting at least part of the red forms absorption.

In the blue region, a strong and broad negative band, with three minima of similar intensity at 498, 474, and 462 nm, characterizes Lhca2. The Lhca3 spectrum in the blue showed two contributions at 467 nm (–) and 500 nm (–).

Protein Complex Stability. The stability of the complexes was measured following the CD signal decay with increasing temperature. The sigmoidal fit of the curves (Figure 6) indicated that the denaturation temperatures for Lhca2 and Lhca3 were of 53.3 ± 1.9 and 45.6 ± 1.4 °C, respectively.

Reconstitution with Different Chl Species. Chlorophyll *b* has been proposed to be involved in the red-shifted spectral forms of LHCI (34). This finding was supported by the loss of red forms upon reconstitution of Lhca4 (35) and Lhca1 (7) with Chl *a* plus xanthophylls but without Chl *b*. It is interesting to assess whether the red forms found in Lhca3, which are quite similar to the ones of Lhca4, are also dependent on the presence of Chl *b*. A positive answer would support a similar origin for red forms in all Lhca gene products. To assess the dependence of the spectral properties of Lhca complexes on Chl *b*, in vitro reconstitution of the Lhca3 complex was performed either in the absence of Chl *b* or in the presence of a Chl *b* excess with respect to the control conditions above-described. Beside, we have reconstituted Lhca4 in the same conditions to obtain comparative results. In the absence of Chl *b*, both proteins yielded a stabile monomer (Lhca3-a; Lhca4-a), which did not contain Chl *b* as assessed by HPLC analysis, but still coordinates Chl *a* and carotenoids. The reconstitution in the presence of excess of Chl *b* also gave a stable product for Lhca4 (Lhca4-b, Chl *a/b* 0.18), while Lhca3 was unstable in these conditions, confirming that this protein requires high Chl *a* occupancy. The absorption and the emission spectra at low temperature of the three holoproteins obtained are presented in Figure 7. The spectra of Lhca3-a were very similar to the spectra of the control Lhca3, with respect to the amplitude of the red forms. The Q_y transition showed a peak at 679 nm, and strong absorption at wavelengths longer than 700 nm was detected. The presence of the red forms was confirmed by the emission spectrum, which showed the maximum at 725 nm (Figure 7A) and a second peak at 685 nm, reproducing the spectrum of the control (see Figure 3B for comparison). In the case of Lhca4-a the situation was different: both absorption and emission showed a decrease in the amplitude of the red

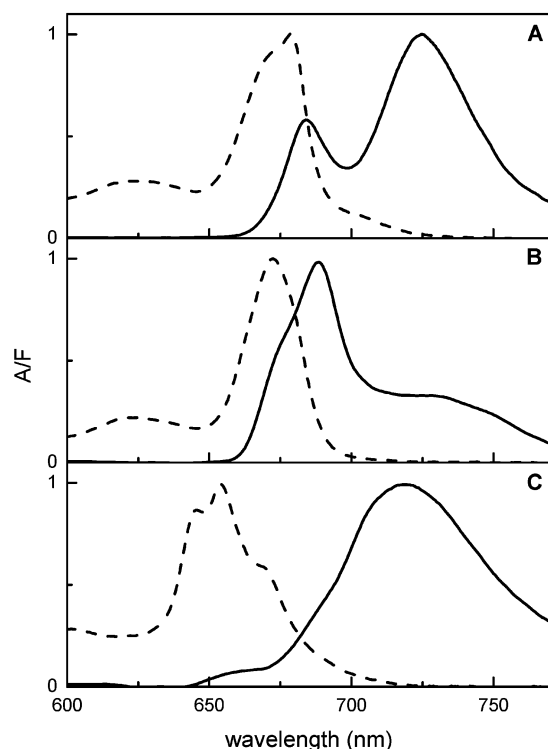


FIGURE 7: Absorption (dashed) and fluorescence emission (solid) spectra at 77 K of Lhca3-a (A), Lhca4-a (B), and Lhca4-b (C).

spectral forms. The fluorescence spectrum showed a 690 nm peak, although a residual weak emission at around 730 nm was still detectable. Moreover, this complex also showed emission contribution around 675 nm, indicating the presence of Chls that do not transfer energy efficiently, and then suggesting that this sample is less stable than the control. The Lhca4-b complex had different spectroscopic properties as compared to both the control and the sample reconstituted with Chl *a* only: its absorption spectrum was characterized by three main bands at 646, 654, and 670 nm, reflecting the high content in Chl *b* (8.5 Chls *b* vs 1.5 Chls *a*), but absorption above 700 nm was still present. The fluorescence emission spectrum showed that most of the energy in this sample is emitted from red-shifted forms, peaking at 719 nm, thus shifted by 11 nm to the blue as compared to the control Lhca4.

DISCUSSION

Lhca2 and Lhca3 are two pigment–protein complex components of the Photosystem I antenna system of higher plants, together with Lhca1 and Lhca4. The predicted size of the Lhca2 polypeptide is of 212 amino acids for a molecular mass of 23 kDa, while Lhca3 is longer (232 AA) and has a molecular mass of 25 kDa (4). Little is at present known about these complexes because of difficulties in purification. The possibility to overexpress the apoproteins in *E. coli* and to reconstitute the complexes in vitro with pigments represents at the moment a unique tool to study the properties of these LHCI subunits. In the following, we discuss the major biochemical and spectroscopic features of Lhca2 and Lhca3 as compared to those of Lhca1 and Lhca4, the two LHCI subunits previously described in detail (7, 18).

Pigment Composition. Pigment/protein stoichiometry measurements on the native LHCI preparation, containing all four

Table 2: Comparison between the Pigment Complements of the Four Lhca Recombinant Complexes^a

sample	Chl <i>a</i>	Chl <i>b</i>	viola	lute	b-car	refs
Lhca1	8 ± 0.04	2 ± 0.04	1.05	1.81		7
Lhca2	6.5 ± 0.2	3.5 ± 0.2	0.47	1.52		this paper
Lhca3	8.6 ± 0.2	1.4 ± 0.2	0.66	1.62	0.57	this paper
Lhca4	7.0 ± 0.2	3 ± 0.2	0.5	1.5		7

^a The number of Chls was determined on the basis of the Chl/Car ratio (see text). The values reported indicate the number of pigments per polypeptide.

Lhca complexes, have shown that 10 Chls are bound in average to each Lhca protein. The analysis of Lhca1 and Lhca4 monomers reconstituted in vitro actually indicated that both complexes coordinate 10 Chls (7) (Table 2). Therefore, a similar stoichiometry is expected for Lhca2 and Lhca3. In all antenna complexes analyzed so far, an integer number of tightly bound carotenoids has always been observed, either two or three depending on the protein (36). The Chl/Car ratio of Lhca2 is 5.0, then assuming a Chl to polypeptide stoichiometry of 10, the complex would accommodate exactly two xanthophylls. In Lhca3, the Chl/Car ratio is 3.4, which would be consistent with the binding of three carotenoids per polypeptide. On the basis of these observations, we propose that each Lhca2 and Lhca3 monomeric complex binds 10 Chls and respectively two and three xanthophyll molecules.

A similar study on the pigment complement of Lhca complexes was recently performed on tomato Lhca complexes (22). Although the results are consistent, differences between the data presented here and the ones by Schmidt and co-workers can be appreciated, especially in the complement of carotenoid binding to each gene product. Discrepancies may be due to species-specific differences as we clearly show in the case of *Zea mays* versus *A. thaliana* LHCI preparations (7). Another source of variability can be the different methods used for the purification of the reconstituted complex from unspecifically bound pigments following reconstitution (cfr. refs 22 and 7).

The primary structure analysis indicates that all the residues, which have been proven to be Chl binding ligands in Lhcb1, are conserved in the Lhca2 and Lhca3 proteins. The only difference is the substitution of glutamine with glutamate as a ligand for Chl B6. This is likely to be a conservative substitution since it was previously shown that Glu can coordinate Chl in both CP29 and Lhca1 (21, 37). In the case of Lhca3, an additional substitution is found at the putative Chl A5 binding site whose binding residue is asparagine, while histidine is found at this position in all Lhc complexes but Lhca4. The Asn versus His substitution was previously reported to be a conservative change for site A2 in Lhcb1 versus Lhcb4 since both amino acid residues were found to be active in the coordination of Chl *a* chromophores. We conclude that Chl binding sites A1, A2, A3, A4, A5, B3, B5, and B6 are present in both Lhca2 and Lhca3. On the basis of sequence analysis, we also suggest that a ninth Chl is accommodated in site B2. In fact, mutation analysis of LHCI has shown that Chl B2 is coordinated via the Chl ligand in site A2 (11, 38) when asparagine is the ligand of Chl A2 (as in Lhcb1, Lhcb5, and Lhca1), while site B2 is empty when histidine is the A2 ligand as in the case of Lhcb4 (21, 37, 38). It was suggested that Chl A2

may assume different orientations, which allows (Asn) or inhibits (His) in the coordination of the additional Chl in site B2 (32). Identification of the location for the tenth Chl ligand can only be tentative. In Lhca1, a Chl binding site has been proposed to be located near Chl A4 (21). Because of the high homology between Lhca proteins, it is possible that this Chl is present in all Lhca complexes.

The carotenoid composition of Lhca2 and Lhca3 is similar except for the presence of β -carotene in Lhca3 (0.5 molecules per polypeptide). The main xanthophyll is lutein, accounting for 1.5 and 1.65 molecules per polypeptide in Lhca2 and Lhca3, respectively, while 0.5 molecules of violaxanthin per monomer were found in Lhca2 versus 0.7 in Lhca3 (Table 2).

The analysis of the Lhcb antenna complexes has identified four carotenoid binding sites. Two of these sites, namely L1 and L2, are located in the center of the molecule and are occupied in all Lhc complexes analyzed so far (11, 36). The third site, N1, located in the C-helix domain, is available only in LHCII and possibly in Lhca1 complex (21, 39), while the loosely binding fourth site, V1, was so far only found in LHCII (40, 41). It seems thus likely that Lhca2 accommodates its two xanthophylls in sites L1 and L2. Site L1 has been shown to be occupied by lutein in all Lhc proteins so far analyzed. The high amount of lutein detected in Lhca2 is consistent with lutein occupancy of site L1 in this protein.

Three carotenoids are coordinated to Lhca3. While it is likely that two of them are accommodated in the L1 and L2 sites, the localization of the third xanthophyll can be discussed. Two sites are the possible candidates: location in site N1 would yield a strong red-shift of the ligand spectrum and an efficient energy transfer to Chl (42), while location in site V1 (40, 41, 43) would induce a smaller spectral shift without energy transfer to Chl *a*. The analysis of the excitation spectrum of Lhca3 revealed that one xanthophyll molecule, absorbing around 485–489 nm, does not transfer energy to Chls. This picture fits the characteristics for site V1 described in LHCII (41) thus suggesting this is the site occupied in the Lhca3 monomer. Although this third carotenoid is not active in light-harvesting, its binding to the complex appears to be rather specific: in fact, this site is able to exclude neoxanthin, which was present in the reconstitution mixture, from binding.

Recombinant versus Native. The Chl *a/b* ratio of the native LHCI preparation from *A. thaliana*, which contains all four Lhca complexes, is 3.3 (30.7 Chls *a* and 9.3 Chls *b* in a minimal unit including one polypeptide for each of the four Lhca) (7). Lhca1 and Lhca4 have been previously reconstituted in vitro using the same procedure here applied to Lhca2 and Lhca3. This led to recombinant proteins with a Chl *a/b* ratio of 4 and 2.3, respectively (see Table 2 for a summary of the pigment complement of the Lhca complexes) (7). Allowing for the presence of an identical number of individual Lhca per P700, we can calculate an averaged Chl *a/b* ratio for the reconstituted complexes of 3.04 (30.1 Chls *a* and 9.9 Chls *b*), which closely reproduces the value obtained on the native LHCI purified from chloroplasts (7).

Similar calculation for carotenoids shows that the four recombinant complexes bind together 10 carotenoid molecules, while nine were found to be associated to the native LHCI preparation. Possible explanations for this discrepancy include: (i) the native complexes are present in dimeric form,

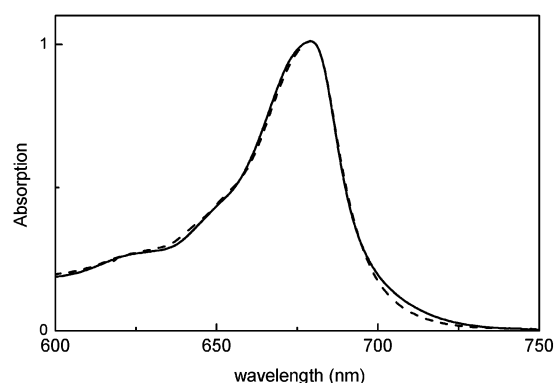


FIGURE 8: Comparison between absorption spectrum of the LHCI native fraction (solid) and the sum of Lhca2 and Lhca3 reconstituted monomers (dashed). The spectra of Lhca2 and Lhca3 normalized to the protein content before performing the sum.

while calculation is based on recombinant monomers. It is thus possible that the third xanthophyll-binding site of Lhca3 is occupied in monomers but not in the native dimers. (ii) Alternatively, we note that detergent treatment removes the xanthophyll in the site V1 of LHCII. Considering that the purification of native LHCI antennas requires harsh detergent treatment (0.5% zwittergent + 1% DM) and repeated freezing–thawing, it is likely that this site can be emptied in the purification of the native complex.

Previous comparison of the native LHCI preparation with the recombinant Lhca1-4 dimer has suggested that the sum of the spectroscopic properties of Lhca2 and Lhca3 has to be similar to that observed for the native LHCI preparation (7). The comparison of the absorption spectra is presented in Figure 8, where the sum of Lhca2 and Lhca3 spectra, obtained upon normalization to the protein concentration, is compared to the spectrum of the native preparation from *A. thaliana* (7). The two spectra are practically identical except for the range above 700 nm, where the native complex shows higher amplitude in the red tail. This difference can be ascribed to the fact that here we are analyzing monomers, while in the native preparation all complexes are in dimeric form. This is consistent with the previous finding that dimerization of Lhca1 and Lhca4 seems to increase the amplitude of the red-shifted spectral forms (7).

Red Forms. The absorption spectra of Lhca2 and Lhca3 are characterized by significant amplitude in the low energy tail, indicating the presence of red spectral Chl forms. This red tail is more pronounced in Lhca3 as compared to Lhca2, suggesting that the energy levels and/or the amplitude of the red forms in the two complexes are different. A similar difference was observed in the case of Lhca1 and Lhca4 proteins, the latter complex exhibiting more intense absorption at lower energy (18). In Figure 9, the absorption spectra at 77 K of the four Lhca complexes are presented. Lhca3 and Lhca4 show an intense red tail, while with different shapes. In Lhca1, the absorption at wavelengths longer than 700 nm is very small, and in Lhca2 a strong absorption component can be detected around 690 nm. Unfortunately, the absorption is structureless in this low energy region and does not allow determining with certainty the properties of each red absorption band. However, information about the energy levels can be obtained from the analysis of the fluorescence emission spectra, in which the contribution at low energy is strongly enhanced. In Figure 10, a comparison

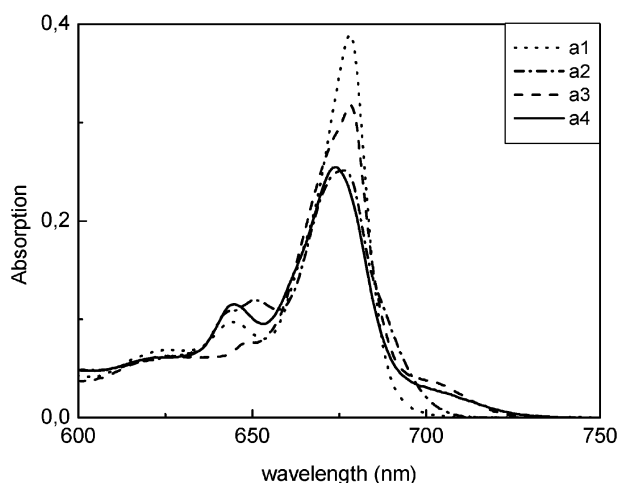


FIGURE 9: Comparison between the absorption spectra at 77 K of Lhca1 (dotted), Lhca2 (dash-dot), Lhca3 (dashed), and Lhca4 (solid). The spectra are normalized to the protein concentration.

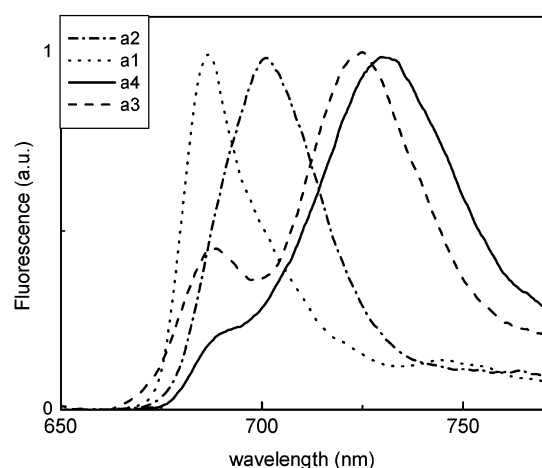


FIGURE 10: Comparison between the fluorescence emission spectra at 77 K of Lhca1 (dotted), Lhca2 (dash-dot), Lhca3 (dashed), and Lhca4 (solid). The spectra are normalized to the maximum.

of the fluorescence emission spectra at low temperature of the four Lhca complexes is presented. The emission peaks at 77 K of Lhca complexes are 686 nm for Lhca1, 701 nm for Lhca2, 725 nm for Lhca3, and 730 nm for Lhca4. Contributions at 701 nm for Lhca1, at 688 nm for Lhca2, and at 685–690 nm for both Lhca3 and Lhca4 can also be detected. It is thus clear that, although red forms are a common characteristic of the Lhca branch of Lhc family, their energy levels and their intensities differ in each complex. This heterogeneity may derive from different mechanisms: (i) the low energy absorptions originate in all complexes from the same pigment pool, and the differences in transition energies and/or intensities of the red forms in each complex are modulated by small changes in the protein/chromophore environment; (ii) two pigment pools, located in different protein environments, are responsible for the red emissions at 701–702 and 725–730 nm, and while in Lhca1 and Lhca2 only the higher energy form is present, in Lhca3 and Lhca4 both are present. Mutational analysis of Lhca1 indicates that the low energy forms of this complex originate from interactions between Chls in the domain formed by sites A5, B5, and B6 (21). The decrease of red forms upon mutation at site B5 and deletion of the N-terminal in Lhca4 suggest that the same domain is responsible for the low

energy absorption in Lhca4 (44, 45). While these results seem to indicate that the Chls absorbing at low energies are accommodated in the same sites in all Lhca complexes, more detailed analysis is required to support this hypothesis.

Role of Chl *b* in the Red Forms. It has been proposed that the large bathochromic spectral shifts of red forms may be due to strong Coulombic interactions between Chl molecules, leading to excitonic band splitting, with the red forms representing the low energy excitonic band of a Chl dimer (46–48). In the case of Lhca4, it has been shown that reconstitution in the absence of Chl *b* yields a complex that does not contain red forms, and it was proposed that Chl *b* can be one of the terms of the interaction leading the low energy absorption (35). Here we have performed the same experiment for Lhca3, which shows an intense red emission and used Lhca4 as control. Besides, we have also obtained a Lhca4 complex binding excess of Chl *b*. The choice of using a low Chl *a/b* ratio instead of reconstituting with only Chl *b* is based on preliminary experiments that have shown that reconstitution in the total absence of Chl *a* does not yield stable complexes for Lhca3 and Lhca4 (22, 35). In the case of Lhca3, neither the reconstitution with Chl *b* only (22) nor the complex in which Chl *b* is in strong excess (Chl *a* is still present in limiting amounts) yielded a folded protein. This indicates that several Chl binding sites need to be occupied by Chl *a* to obtain a stabilization of the complex. Reconstitution with only Chl *a* gives a stable product, which has properties similar to the control sample, in particular with respect to energy and amplitude of the red forms thus showing that Chl *b* does not play any role in determining the red absorption of Lhca3.

The situation appears different in the case of Lhca4. The sample reconstituted with only Chl *a* shows the emission maximum at 690 nm, but red emission at 730 nm is still detectable, although less intense than in the control sample. The presence of the 730 nm emission in Lhca4-a indicates that this form originates from Chl *a* molecules. The ratio between the emissions from the bulk and the red forms suggests that the preparation of Lhca4-a is heterogeneous. In fact, because of the high energetic difference between the bulk and the low energy forms, it is expected, for an equilibrated system, that the energy is emitted from the red forms. This is not the case at 77 or at 4 K (35), clearly indicating that there are at least two populations in the sample, one containing red forms, and the other depleted of this property. The presence of at least two conformations, having different fluorescence lifetimes, was previously described in the case of Lhc complexes (49). In Lhca4-a, the changes in the bound chromophores may have affected the equilibrium between the two conformations thus stabilizing the conformation with lower wavelength emission.

When Lhca4 is reconstituted with an excess of Chl *b* (Lhca4-b), the emission is still red, although the maximum is shifted 11 nm to the blue as compared to the control. This difference can be easily explained by hypothesizing that one of the two Chls *a* chromophores interacting in the control complex is substituted by a Chl *b* in Lhca4-b. Even in the case that the two Chls maintain the same relative distance, the same geometry, and the other partner of the interaction (a Chl *a*) has the same monomeric absorption as in the control sample, the presence of the Chl *b* as a second member of the interaction would reduce the excitonic shift in the

absorption because of two factors: (i) the value for the transition moment for Chl *b* is smaller than for Chl *a*, and this would reduce the value of the interaction strength (*J*); (ii) because of the larger energetic distance between the two monomers, the shift of each forms would be smaller. Another possible explanation is that the 719 nm emission form is already present in the control Lhca4 complex and that in the Lhca4-b the red most shifted forms, originating the 730 nm emission, is lost. This seems unlikely since the 719 nm emission was never detected in previous work (15, 19). However, this possibility cannot be ruled out at present.

The maintaining of the Chl–Chl interactions responsible for red-shifted forms in Lhca4-b despite major changes in the sites occupancy, while in the Lhca4-a complex these are strongly reduced and the complex destabilized, suggests that the role of Chl *b* is structural. The presence of a Chl *b* in one of the sites (possibly B6 according to the mutational analysis of Lhca1 (21)) is needed to keep the complex in the right conformation leading to the red forms. It is interesting to note that the stability of Lhca3 and Lhca4 proteins exhibiting strong red-shifted fluorescence emission is substantially lower (by approximately 10°) with respect to Lhca1 and Lhca2, while this effect does not depend on the number of carotenoids bound to each holoprotein. It thus appears that the maintaining of the special pigment–pigment interactions requires the adoption of a less stable conformation.

Do Lhca2 and Lhca3 Form Homo- or Heterodimers? It has been shown that all Lhca complexes are dimers in vivo (7). While in vitro reconstitution has shown that Lhca1 and Lhca4 forms heterodimers and that the energy is efficiently transferred from one subunit to the other (18, 20), it is at present not known whether Lhca2 and Lhca3 form homo- or heterodimers. Reconstitution of Lhca2 and Lhca3, in the same conditions leading to the formation of Lhca1-4 heterodimer, does not induce dimerization of these complexes (22), probably indicating that an unknown component is needed to stabilize the dimer but leaving the question open. Ihalainen et al. (15) showed that two low energy emitters at 702 and 730 nm, respectively, were present in the LHCI preparation containing all four complexes. The 730 nm emission was assigned to the Lhca1-4 heterodimer, in agreement with previous data, while the 702 nm was assigned to Lhca2 and/or Lhca3 homo/heterodimer(s).

The data in the present work show that the 701 nm emission originates from Lhca2 complex, while Lhca3 shows emission at 725 nm. If a heterodimer would be formed between these two complexes, then only the 725 nm emission is expected in the native preparation because of effective energy transfer between the two subunits as observed for the Lhca1-4 complex. The fact that the 702 nm component is detectable in the LHCI native preparation, where all complexes are in dimeric form, suggests that at least part of the Lhca2 and Lhca3 population forms a homodimer. This hypothesis is supported by the analysis of the lifetime decay of the LHCI native preparation (16) that suggests the presence of three different types of dimers.

CONCLUSIONS

In this work, we have obtained recombinant Lhca2 and Lhca3 holoprotein by refolding apoproteins overexpressed in *E. coli* with purified pigments. The pigment–protein

complexes were characterized for their biochemical and spectroscopic properties allowing a comparative study of the four gene product components of LHCI. These proteins are able to modulate the absorption/emission properties of specific Chls and to produce red-shifted spectral forms. While this seems to be a characteristic of all Lhca, it appears that the amplitude and the transition energy of these forms are different in the four complexes. Reconstitution of Lhca3 and Lhca4 with different Chl complements led to the conclusion that the red absorption originates from interaction between Chl *a* molecules and that any direct or indirect involvement of Chl *b* can be excluded for Lhca3. In Lhca4, Chl *b* may contribute to stabilization of a protein conformation allowing for the right geometry between Chl *a* molecules involved in the excitonic interaction yielding to red forms.

REFERENCES

- Mullet, J. E., Burke, J. J., and Arntzen, C. J. (1980) *Plant Physiol.* 65, 814–822.
- Bassi, R., Machold, O., and Simpson, D. (1985) *Carlsberg Res. Commun.* 50, 145–162.
- Bassi, R., and Simpson, D. (1987) *Eur. J. Biochem.* 163, 221–230.
- Jansson, S. (1999) *Trends Plant Sci.* 4, 236–240.
- Damm, I., Steinmetz, D., and Grimme, L. H. (1990) in *Current research in photosynthesis* (Baltscheffsky, M., Ed.) pp 607–610, Kluwer Academic Publishers, Dordrecht, The Netherlands.
- Croce, R., and Bassi, R. (1998) in *Photosynthesis: Mechanisms and Effects* (Garab, G., Ed.) pp 421–424, Kluwer Academic Publishers, Dordrecht, The Netherlands.
- Croce, R., Morosinotto, T., Castelletti, S., Breton, J., and Bassi, R. (2002) *Biochim. Biophys. Acta* 1556, 29–40.
- Boekema, E. J., Jensen, P. E., Schlodder, E., van Breemen, J. F., van Roon, H., Scheller, H. V., and Dekker, J. P. (2001) *Biochemistry* 40, 1029–1036.
- Jensen, P. E., Gilpin, M., Knoetzel, J., and Scheller, H. V. (2000) *J. Biol. Chem.* 275, 24701–24708.
- Scheller, H. V., Jensen, P. E., Haldrup, A., Lunde, C., and Knoetzel, J. (2001) *Biochim. Biophys. Acta* 1507, 41–60.
- Kühlbrandt, W., Wang, D. N., and Fujiyoshi, Y. (1994) *Nature* 367, 614–621.
- Green, B. R., and Pichersky, E. (1994) *Photosynth. Res.* 39, 149–162.
- Lam, E., Ortiz, W., and Malkin, R. (1984) *FEBS Lett.* 168, 10–14.
- Tjus, S. E., Roobol-Boza, M., Palsson, L.-O., and Andersson, B. (1995) *Photosynth. Res.* 45, 41–49.
- Ihalainen, J. A., Gobets, B., Sznee, K., Brazzoli, M., Croce, R., Bassi, R., van Grondelle, R., Korppi-Tommola, J. E. I., and Dekker, J. P. (2000) *Biochemistry* 39, 8625–8631.
- Gobets, B., Kennis, J. T. M., Brazzoli, M., Croce, R., van Stokkum, I. H., Bassi, R., Dekker, J. P., Van Amerongen, H., Fleming, G. R., and van Grondelle, R. (2001) *J. Phys. Chem. B* 105, 10132–10139.
- Plumley, F. G., and Schmidt, G. W. (1987) *Proc. Natl. Acad. Sci. U.S.A.* 84, 146–150.
- Schmid, V. H. R., Cammarata, K. V., Bruns, B. U., and Schmidt, G. W. (1997) *Proc. Natl. Acad. Sci. U.S.A.* 94, 7667–7672.
- Melkozernov, A. N., Schmid, V. H. R., Schmidt, G. W., and Blankenship, R. E. (1998) *J. Phys. Chem. B* 102, 8183–8189.
- Melkozernov, A. N., Lin, S., Schmid, V. H. R., Paulsen, H., Schmidt, G. W., and Blankenship, R. E. (2000) *FEBS Lett.* 471, 89–92.
- Morosinotto, T., Castelletti, S., Breton, J., Bassi, R., and Croce, R. (2002) *J. Biol. Chem.* 277, 36253–36261.
- Schmid, V. H. R., Potthast, S., Wiener, M., Bergauer, V., Paulsen, H., and Storf, S. (2002) *J. Biol. Chem.* 277, 37307–37314.
- Knoetzel, J., Svendsen, I., and Simpson, D. J. (1992) *Eur. J. Biochem.* 206, 209–215.
- Zhang, H., Goodman, H. M., and Jansson, S. (1997) *Plant Physiol.* 115, 1525–1531.
- Ganeteg, U., Strand, A., Gustafsson, P., and Jansson, S. (2001) *Plant Physiol.* 127, 150–158.

26. Sambrook, J., Fritsch, E. F., and Maniatis, T. (1989) *Molecular cloning. A laboratory manual*, Cold Spring Harbor Laboratory Press, Woodbury, NY.
27. Nagai, K., and Thøgersen, H. C. (1987) *Methods Enzymol.* 153, 461–481.
28. Paulsen, H., and Hobe, S. (1992) *Eur. J. Biochem.* 205, 71–76.
29. Giuffra, E., Cugini, D., Croce, R., and Bassi, R. (1996) *Eur. J. Biochem.* 238, 112–120.
30. Gilmore, A. M., and Yamamoto, H. Y. (1991) *Plant Physiol.* 96, 635–643.
31. Croce, R., Canino, G., Ros, F., and Bassi, R. (2002) *Biochemistry* 41, 7343.
32. Giuffra, E., Zucchelli, G., Sandona, D., Croce, R., Cugini, D., Garlaschi, F. M., Bassi, R., and Jennings, R. C. (1997) *Biochemistry* 36, 12984–12993.
33. Croce, R., Cinque, G., Holzwarth, A. R., and Bassi, R. (2000) *Photosynth. Res.* 62, 221–231.
34. Mukerji, I., and Sauer, K. (1990) *Curr. Res. Photosynth.* 2, 321–324.
35. Schmid, V. H., Thome, P., Ruhle, W., Paulsen, H., Kuhlbrandt, W., and Rogl, H. (2001) *FEBS Lett.* 499, 27–31.
36. Sandona, D., Croce, R., Pagano, A., Crimi, M., and Bassi, R. (1998) *Biochim. Biophys. Acta* 1365, 207–214.
37. Bassi, R., Croce, R., Cugini, D., and Sandona, D. (1999) *Proc. Natl. Acad. Sci. U.S.A.* 96, 10056–10061.
38. Remelli, R., Varotto, C., Sandona, D., Croce, R., and Bassi, R. (1999) *J. Biol. Chem.* 274, 33510–33521.
39. Croce, R., Remelli, R., Varotto, C., Breton, J., and Bassi, R. (1999) *FEBS Lett.* 456, 1–6.
40. Ruban, A. V., Lee, P. J., Wentworth, M., Young, A. J., and Horton, P. (1999) *J. Biol. Chem.* 274, 10458–10465.
41. Caffarri, S., Croce, R., Breton, J., and Bassi, R. (2001) *J. Biol. Chem.* 276, 35924–35933.
42. Croce, R., Muller, M. G., Bassi, R., and Holzwarth, A. R. (2001) *Biophys. J.* 80, 901–915.
43. Croce, R., Weiss, S., and Bassi, R. (1999) *J. Biol. Chem.* 274, 29613–29623.
44. Schmid, V. H. R., Paulsen, H., and Rupprecht, J. (2002) *Biochemistry* 41, 9126–9131.
45. Rupprecht, J., Paulsen, H., and Schmid, V. H. R. (2001) *Photosynth. Res.* 63, 217–224.
46. Gobets, B., Van Amerongen, H., Monshouwer, R., Kruip, J., Rögner, M., van Grondelle, R., and Dekker, J. P. (1994) *Biochim. Biophys. Acta* 1188, 75–85.
47. Savikhin, S., Xu, W., Soukoulis, V., Chitnis, P. R., and Struve, W. S. (1999) *Biophys. J.* 76, 3278–3288.
48. Engelmann, E., Tagliabue, T., Karapetyan, N. V., Garlaschi, F. M., Zucchelli, G., and Jennings, R. C. (2001) *FEBS Lett.* 499, 112–115.
49. Moya, I., Silvestri, M., Vallon, O., Cinque, G., and Bassi, R. (2001) *Biochemistry* 40, 12552–12561.

BI027398R